Investigation on thermal performance of the wall-mounted attached ventilation for night cooling under hot summer conditions

Ji, Wenhui; Luo, Qing; Zhang, Zili; Wang, Houhua; Du, Tao; Heiselberg, Per Kvols

Published in:
Building and Environment

DOI (link to publication from Publisher):
10.1016/j.buildenv.2018.10.002

Publication date:
2018

Document Version
Accepted author manuscript, peer reviewed version

Accepted Manuscript

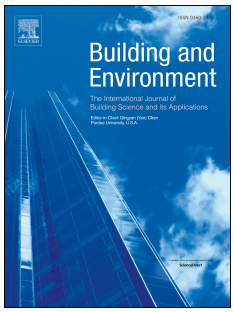

Investigation on thermal performance of the wall-mounted attached ventilation for night cooling under hot summer conditions

Wenhui Ji, Qing Luo, Zili Zhang, Houhua Wang, Tao Du, Per Kvols Heiselberg

PII: S0360-1323(18)30614-0

DOI: 10.1016/j.buildenv.2018.10.002

Reference: BAE 5732

To appear in: *Building and Environment*

Received Date: 6 July 2018

Revised Date: 30 September 2018

Accepted Date: 1 October 2018

Please cite this article as: Ji W, Luo Q, Zhang Z, Wang H, Du T, Heiselberg PK, Investigation on thermal performance of the wall-mounted attached ventilation for night cooling under hot summer conditions, *Building and Environment* (2018), doi: https://doi.org/10.1016/j.buildenv.2018.10.002.

Investigation on thermal performance of the wall-mounted attached ventilation for night cooling under hot summer conditions

Wenhui Ji [a, b], Qing Luo [a, b], Zili Zhang [c*], Houhua Wang [a, b], Tao Du [a, b], Per Kvols Heiselberg [d]

[a] *Department of Urban Construction and Environmental Engineering, Chongqing University, Chongqing 400045, China*

[b] *Key Laboratory of the Three Gorges Reservoir Region's Eco-Environment, Ministry of Education, Chongqing 400045, China*

[c] *Department of Engineering, Aarhus University, Aarhus 8000, Denmark*

[d] *Department of Civil Engineering, Aalborg University, Aalborg 9220, Denmark*

Abstract: In Hot Summer and Cold Winter Climate Zone, the cooling potential of natural/passive night ventilation is limited during summer due to the insignificant difference between the outdoor and indoor temperatures. Therefore, a novel mechanical ventilation strategy, the wall-mounted attached ventilation (WAV) system, is proposed in the present paper to improve ventilation efficiency of night cooling. The idea is that WAV can produce a downward airflow over the internal wall surface that is somewhat similar to a sidewall jet, so as to achieve enhanced heat transfer in the room. This paper starts with a series of experiments in a test chamber, and continues with thermal analysis of the heat transfer characteristics and heat removal performance of WAV. The performance of night ventilation with WAV is further evaluated in terms of ventilation efficiency index and energy performance index. It is shown that the overall average value of the convective heat transfer coefficient at the internal wall surface with WAV is 10.79 W m^{-2} ℃$^{-1}$. With WAV, the amount of heat removed from the ventilated wall is about five times that in the natural night ventilation case, and the total amount of heat removed from the whole

* Corresponding author.
Email address: zili_zhang@eng.au.dk (Zili Zhang)

chamber is twice as much. The average value of the surface cooling effectiveness of WAV is 1.48, and the overall coefficient of performance (COP) of WAV turns out to be 26.8. As a night ventilation strategy, WAV is capable to achieve good cooling performance under hot summer conditions.

Keywords**:** night ventilation; wall-attached jet; convective heat transfer; heat removal; temperature efficiency

Nomenclature

a	Thermal diffusivity (m^2 s^{-1})
A	Surface area (m^2)
ACR	Air change rate (ACH)
c	Specific heat conductivity (J kg^{-1} K^{-1})
d	Thickness (m)
Fo	Fourier number
$F_{s,p}$	View factor (from surface s to surface p) (-)
h	Convective heat transfer coefficient (W m^{-2} K^{-1})
J_s	Radiosity of surface s
k	Time instant
$\dot{m}$	Air flow rate (kg s^{-1})
q	Heat flux (W m^{-2})
Q	Heat removal amount (kJ)
T	Temperature (℃)

ΔT	Temperature difference (℃)
T_{ex}	External surface temperature of the west wall (℃)
T_{in}	Internal surface temperature of the west wall (℃)
T_{inlet}	Inlet air temperature (℃)
T_{outlet}	Outlet air temperature (℃)
T_{room}	Room air temperature (℃)
x	Coordinate along the width of the wall
Δx	Grid size

Greek symbols

ρ	Density (kg m^{-3})
λ	Thermal conductivity (W m^{-1} K^{-1})
ε_s	Emissivity of surface *s* (-)
τ	Time (s)
$\Delta\tau$	Time step (s)
η	Effectiveness (-)
σ	Stefan-Boltzmann constant (5.67 × 10^{-8} W m^{-2} K^{-4})

Subscripts

a	air
cond	Conduction
conv	Convection

extr	Extraction
fan	Electric fan
rad	Radiation
surf	Surface
vent	Ventilation
w	West wall

Abbreviations

APJ	Attached plane jet
CHTC	Convective heat transfer coefficient
CJV	Confluent jet ventilation
IJV	Impinging jet ventilation
WAV	Wall-mounted Attached Ventilation

1. INTRODUCTION

Buildings consume more than 40% of the world's energy and generate nearly one-third of greenhouse gas emissions [1]. In China, due to the policy of promoting urbanization and the requirement of economic development, the total floor area of buildings has reached approximately 57.3 billion square meters in 2015, and still displaying an upward trend [2,3]. Therefore, environmentally sustainable strategies are expected to be applied to maintain indoor comfort with a low level of energy consumption. Night ventilation is an important low-energy approach to adjust the indoor thermal environment and to improve indoor air quality, which is both economic and

environmental-friendly [4][5]. Especially for office buildings, the large heat load at daytime and the non-occupied situation at nighttime provide a good condition for applying the night ventilation strategy. Night ventilation is employed to release the stored heat with cool outdoor air during the night time, and further to provide a certain amount of cooling capacity for the following day. Existing studies show that night ventilation contributes to improving the indoor thermal conditions [6–8] and reducing the cooling load [9], and even completely eliminating the energy consumption of air conditioning under proper climatic conditions [10]. In addition, the application of night ventilation is usually combined with thermal mass [11,12], PCM materials [13,14] and heat recovery air conditioning system [15].

Previous sensitivity studies reveal that the parameters that determine the night cooling effect can be classified into three groups, namely the climatic parameters, the building parameters and the technical parameters [16].

The climatic parameters are related to the environment or climate. The climatic potential of night ventilation is highly dependent on the temperature difference between the outdoor air and room air during the ventilated hours, as well as the diurnal temperature swing which is the difference between maximum daytime and minimum nighttime temperature [17]. In Europe, Artmann et al. [18] propose the climatic cooling potential (CCP) as the index to evaluate the cooling potential of night cooling in all climatic zones of Europe. Results show that there is a very significant cooling potential in Northern Europe, while in relatively warm district night cooling is not sufficient to guarantee thermal comfort thus supplementary strategies are needed. In China, an earlier study [19] on night cooling in Northern China revealed a significant cooling potential, while in Hot Summer and Cold Winter Climate Zone (along the Yangtze River), the application of night cooling should be considered with caution [21,22]. In this Climate Zone, temperature difference between the outdoor air and indoor air during the night is

insignificant in summer time, making it challenging to implement night ventilation in the same way as in other Climate Zones.

The building-specific parameters [23,24] are associated with the physical characteristics such as the building materials, the room geometry, the window types and the internal gains, et al., which should be taken into account when implementing the night ventilation system. Givoni [17] suggests that the characteristics of high-mass, good insulation and shading of a building effectively contribute to the cooling effect of night ventilation. For existing buildings, building-specific parameters act as inputs or constraints for the design/selection of night ventilation systems.

The technical parameters, on the other hand, mainly refer to the airflow pattern, the airflow rate and the operation schedule of night ventilation, all of which have an influence on the heat transfer during night ventilation [25]. Traditionally, the common airflow pattern of mechanical night ventilation is cross ventilation. In the cross ventilation, which is based on Mixing Ventilation (MV) principle, the supply air is blended with the existing room air to ensure uniform air distribution [30]. Both experimental [26] and numerical [23,27] investigations have been performed on the convective heat transfer by the cross ventilation during the night. It provides excellent thermal comfort and large air-conditioned space, but often exhibits poor performance on heat removal [31]. The effects of enclosure shape and positions of openings on the performance of night cooling using cross ventilation have also been studied [28]. More recently, Landsman [29] conducted a comprehensive parametric study of night ventilation including the effect of ventilation schemes, with only the traditional cross ventilation and natural ventilation investigated. Considering that the climatic cooling potential of night ventilation in hot climates is limited, an alternative flow pattern, the jet flow, is considered for improving the cooling efficiency of the night ventilation system.

Previous studies on jet ventilation including Impinging Jet Ventilation (IJV) [32–35]and Confluent Jet Ventilation (CJV) [36–38], have proven that jet flow contributes to enhanced cooling effect as well as better thermal comfort. The IJV method is based on the principle of supplying a high momentum air jet that impinges downward onto the floor. Karimipanah and Awbi [39] carried out both experimental and numerical studies on the performance of the IJV system, and also compared it with displacement ventilation (DV) system, showing slightly better air quality and more uniform velocity distribution due to a better balance between the buoyancy and the momentum forces. Arghand et al. [40] also concluded that the higher air exchange efficiency of the corner-mounted CJV system is suitable for open-plan office environments.

Furthermore, some novel jet flow methods have also been investigated. Cao [41][42] studied the characteristics of ceiling-mounted attached plane jet (APJ), including the mean flow field structure, the specification of jet regions and the maximum velocity decay. Li et al. [43,44] and Yin and Li [45] studied the airflow characteristics of air curtain jets based on the vertical wall jet principle. Recently, Yin et al. [46] conducted experimental studies on the performance of square column attached ventilation. However, the focus of all these previous studies is mainly on the flow properties of different jet ventilation methods, while the thermal performance of jet flow on heat removal is rarely investigated.

The present study aims at evaluating the thermal performance of a novel mechanical ventilation system, the wall-amounted attached ventilation (WAV), for night cooling of an office-type room (with brick walls) located in Chongqing, China. The building parameters are thus specified as: 1) zero internal gain during the night; 2) the brick walls are the primary contribution to the thermal mass. Being part of the Hot Summer and Cold Winter Zone, Chongqing is one of the hottest and most humid

cities in China during summer, and experiences only slightly different outdoor air temperature and indoor air temperature at night. Therefore, the jet ventilation method rather than the cross ventilation method will be preferred for night cooling. Proposed and preliminarily tested by Ji et al. [47–49], the WAV system functions based on the vertical wall-attached jet principle. By introducing the outdoor air over the internal wall surface vertically with a high jet air velocity, enhanced heat transfer is to be expected, which will result in higher efficiency of heat removal from walls during the night cooling period.

The WAV system for night cooling under hot summer conditions is extensively investigated in this paper using both chamber experiments and theoretical thermal analysis models. A series of experiments have been carried out using a rooftop test chamber in natural environment for a total duration of 26 days from June to July 2017. Three cases corresponding to different night ventilation schemes are considered in the experiments for performance comparison, i.e., with WAV, with natural ventilation and without ventilation. Time-varying temperature distributions at different parts of the room are measured together with the velocity fields. Next, for thermal performance analysis and comparison of night ventilation schemes, transient heat transfer models are established to obtain the internal surface convection and the heat extraction from walls. The wall surface temperatures measured from the experiments are used as unsteady boundary conditions for numerically solving the transient heat transfer models. The results show superior thermal performance of WAV comparing with the other two night ventilation schemes, in terms of the amount of heat removed from the ventilated wall and the total amount of heat removed from the chamber. Furthermore, the thermal performance indices and energy performance index of night cooling system with WAV are evaluated.

The paper is organized as follows: methodology including the experimental descriptions and the

thermal analysis model is described in Section 2. Section 3 discusses the experimental results, thermal analysis and performance evaluation of nigh ventilation with WAV. The conclusions are summarized in Section 4. Fig. 1 shows the flow chart of the structure of this paper.

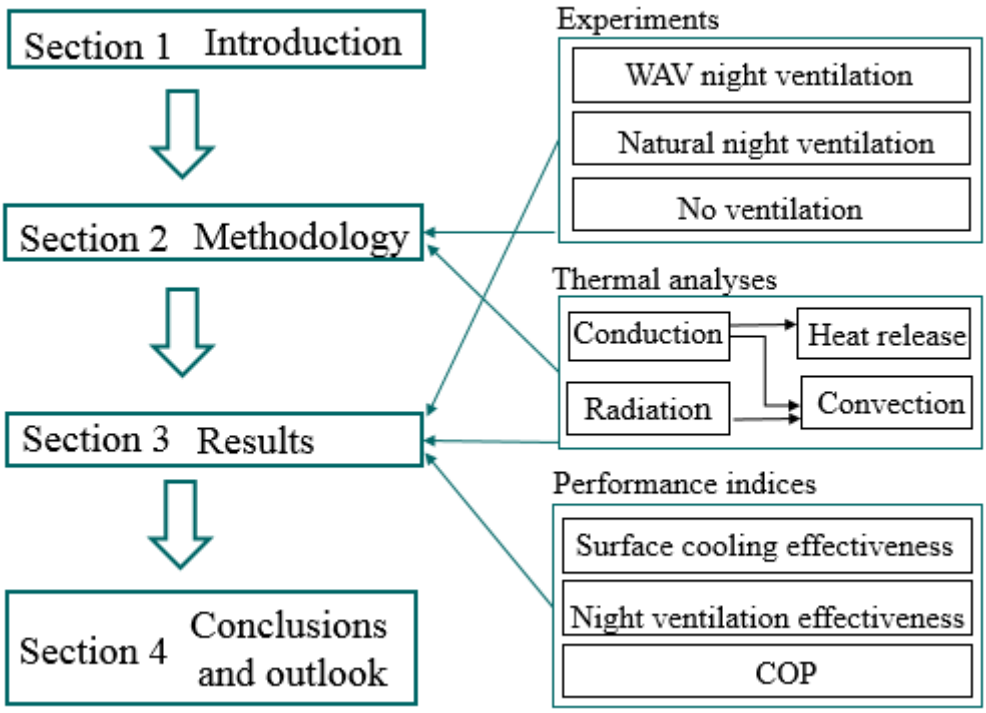

Fig. 1 Flow chart of the structure of this paper

2. Methodology

Both experimental and theoretical investigations have been performed. Experiments at a test chamber provide the temperature distributions on the wall surfaces and in the room, for three different night ventilation schemes. The established transient heat transfer models can be used for thermal performance analysis on night ventilation schemes, with unsteady boundary conditions of the model obtained from the experimental measurements.

2.1 Experiments

2.1.1 Experimental set-up

The experiments have been performed in a rooftop chamber located at the Laboratory of Urban Construction and Environmental Engineering of Chongqing University, Chongqing, China. The internal dimensions of the test room are 3.39 m (length) × 2.81 m (width) × 3 m (height), resulting in a volume of 28.58 m^3. The test chamber has been constructed using double glazed windows and perforated bricks with external thermal mortar as the external insulation. The details of the materials used in the experiments are listed in Table 1.

Table 1

Characteristic of the envelope components of the test chamber (from inside to outside).

Envelope component	Material	d (m)	ρ (kg/m^3)	λ (W/m K)	c (J/kg K)	ε (-)
Roof	Cenment	0.015	1800	0.93	1050	0.65±0.05
	Cystosepiment	0.2	20	0.031	1470	
	Iron sheet	0.002	7272	52	420	
	Cement	0.015	1800	0.93	1050	
Wall	Thermal mortar	0.03	400	0.085	1050	0.88±0.02
	Ceramic concrete hollow brick	0.2	1100	0.334	1050	
	Cement	0.015	1800	0.93	1050	
Floor	Cement	0.015	1800	0.93	1050	0.90±0.05
	Asphalt	0.004	1700	0.5	1000	
	Cement	0.015	1800	0.93	1050	

Envelope component	Material	d (m)	ρ (kg/m^3)	λ (W/m K)	c (J/kg K)	ε (-)
	Reinforced concrete,	0.2	2300	1.9	840	
	Cement	0.015	1800	0.93	1050	

where d, ρ, λ and c are the thickness, density, thermal conductivity and heat capacity of the wall material, respectively, ε is the emissivity of the inner wall surface. As shown in Table 1, each wall has four material layers, which will be taken into account in the conduction model in Section 2.2.2.

Fig. 2 depicts the chamber with the WAV system. The four different material layers of each wall are clearly illustrated in Fig. 2(a). The basic design of the ventilation scheme for generating the attached wall jet is as follows: outdoor air is supplied into the air duct driven by a ventilation fan. The wall-attached air jet is generated by supply air flowed vertically over the inner surface of the west wall from a long and narrow slot (4 in Fig. 2) at the bottom of the air duct (3 in Fig. 2). A square hole in the north wall is used as the inlet opening (1 in Fig. 2) and is placed at a position which is 2.6 m above the floor. The ventilation fan is installed in the inlet opening with sealant around the edges to keep the air flow rate constant while the fan is running. The supply air flow rate is regulated by a speed controller and is kept constant under the working condition of ventilation. Since the test chamber is located in real outdoor environment, the supply air temperature is not manually controlled, and it varies following the change of outdoor air temperature changes. Furthermore, another hole with an area of 0.4 m × 0.4 m in the east wall is used as the outlet opening (5 in Fig. 2). The air is drawn from the chamber through the outlet opening by the pressure difference between the indoor and outdoor environments.

The properties of the ventilation system are:

- The supply duct has a height of 2.7 m above the floor;
- The supply duct has an area of 0.25 m × 0.2 m and a length of 3 m;
- The slot opening has an area of 0.02 m× 2.6 m.

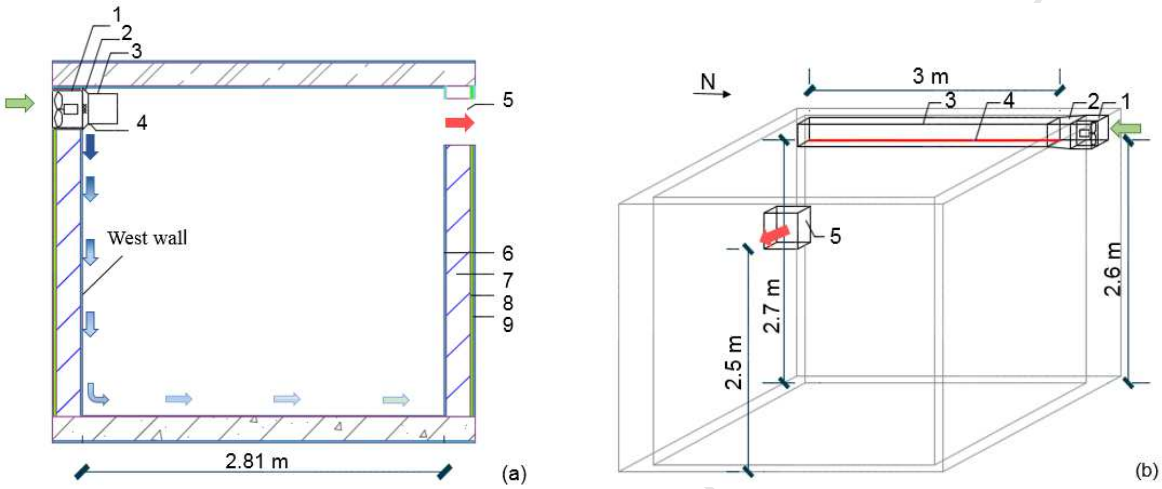

Fig. 2. The test chamber with the WAV system. (a) cross-section view; (b) 3-D view. (1. Axial fan; 2. Flexible connection; 3. supply air duct; 4. Supply slot; 5. Outlet opening; 6. Cement; 7. Brick; 8. Insulation; 9. Cement).

2.1.2. Three cases with different ventilation schemes

The measurement period is from June 27, 2017 to July 23, 2017 (totally 26 days). For each case, measurement is started at 8:00 am and ended at 8:00 the next morning with a duration of 24 hours. Three difference cases with different night ventilation schemes have been investigated as shown in Table 2, i.e., case 1 with WAV, case 2 with natural night ventilation, and case 3 without ventilation (door and windows closed). For the WAV case, the inlet air velocity is kept constant at 5.82 m/s. For the natural night ventilation case, the northern window is opened from 22:00 to 8:00, and the outlet is also kept open during the night. For Case 3, the door and windows of the test chamber are closed for all 24 hours.

Since the outdoor air is directly supplied into the chamber during night ventilation, the real

cooling effects of the three ventilation schemes can be realistically investigated. On the other hand, the outdoor surroundings and thus the supply air temperature cannot be controlled. In order to make fair comparisons of these three cases, results from three days (July 12th for case 1, July 17th for case 2 and July 21th for case 3) with similar outdoor environment have been selected for further analysis and comparison. The recorded variations of the outdoor dry bulb air temperature and relative humidity for these three days are presented in Fig. 3.

Table 2

Experimental conditions for the three different cases

Case	Date	Outdoor air temperature (°C)	Ventilation scheme	Average inlet air velocity (m/s)	ACR (h^{-})	Fan power consumption (W)
1	July 12th	32.01±4.68	WAV 22:00–8:00	5.82	10.27	40
2	July 17th	32.04±4.52	Natural night ventilation 22:00–8:00	-	1.14	-
3	July 21th	33.1±5.35	No ventilation	-	-	-

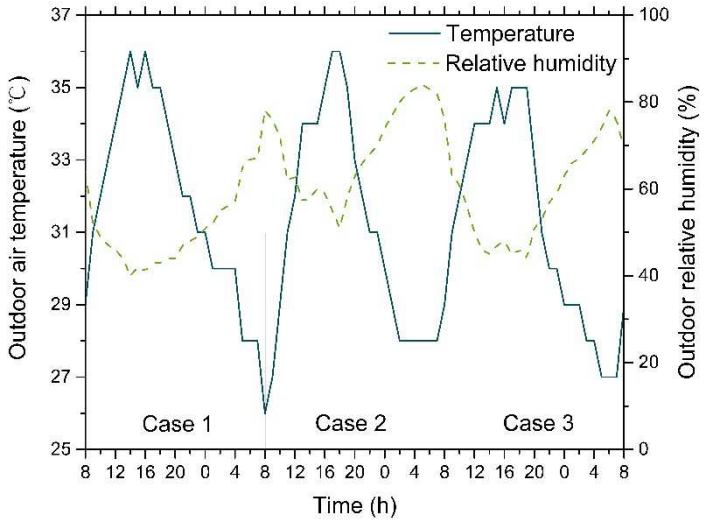

Fig. 3. Outdoor dry bulb air temperature and relative humidity

2.1.3. Measurements

The following parameters have been measured for all three cases:

- external and internal wall surface temperatures,
- dry bulb air temperature and humidity of the outdoor environment and the indoor air,
- temperatures and velocities of the supply air, the duct air, the exhaust air, the room air,
- power consumption of the supply fan.

The outdoor air temperature and the relative humidity are measured and recorded by a Tinytag automatic recorder located 2.4 m above the ground outside the chamber with rain and radiation protections. To determine the cooling effect of different night ventilation schemes, both external and internal surface temperatures have been measured with totally 40 type T thermocouples attached on walls from each orientation of the test chamber, as shown in Fig. 4(a). In order to obtain the temperature variation with time, the sampling period of each thermocouple is set to be 60 s, and data are logged by an Agilent data logger. Fig. 4(b) shows that totally five thermal anemometers are placed at three different heights of the central plane of the chamber to measure the room air temperature. Moreover, the air temperatures and velocities of the supply air, the inlet air and the exhaust air have been recorded using anemometers. All the sensors have been calibrated before installation.

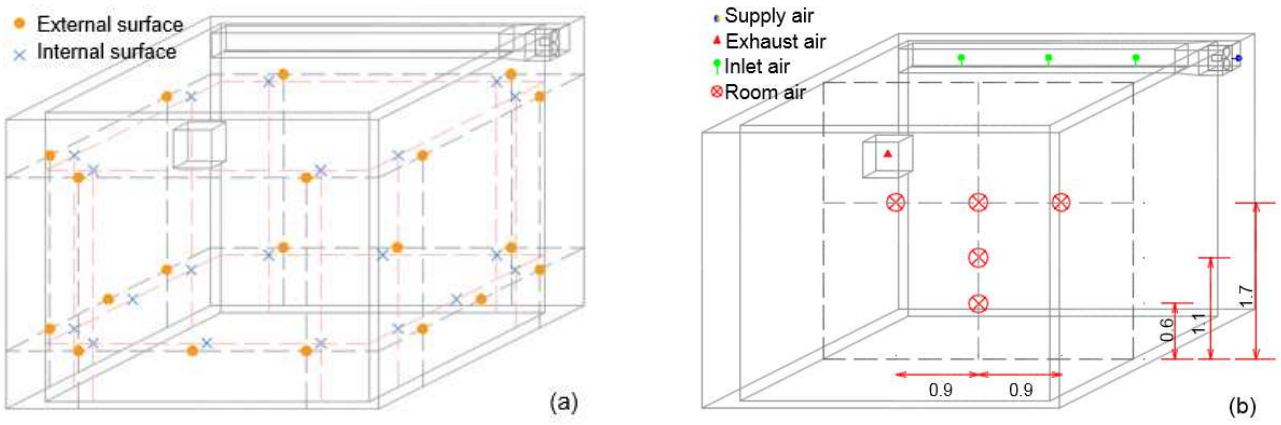

Fig. 4. Location of sensors detecting: (a). wall surface temperatures; (b) air temperatures and velocities at the inlet and outlet, in the supply duct and in the room.

Furthermore, the power consumption of the supply fan is measured using a power meter which has been checked by the installation company. The result of fan power has been given in Table 2.

Finally, the accuracy and range of the measuring instruments used in the present study are summarized in Table 3.

Table 3

The accuracy and range of the instrumentation used in this study.

Measured parameter	Instrument	Range	Accuracy
Temperature	Type T thermocouple	-50 ℃ to +500 ℃	±0.15 ℃
Air velocity	Testo thermal anemometer	0 to 20 m/s	±0.03 m/s
Local climate	Tinytag data recorder	−25 ℃ to +85℃; 0–95% RH	±0.2 ℃; ±3% RH
Power consumption	Multifunction power meter	0.01 kW to 600 kW	±3%

2.2. Transient heat transfer model for thermal analysis

2.2.1 General description of the model

The test chamber is not adiabatic. Fig. 5 shows the schematic representation of the heat transfer on the west wall during the night. The *x* axis is defined along the wall width with its positive direction pointing from the external surface towards the internal surface. *x*=0 and *x*=*d* correspond to the external surface and internal surface, respectively, where *d* is the wall width. During the night ventilation (22;00 to 8:00), the external wall surfaces are cooled by night-time sky radiation as well as convection between outdoor air and external wall surfaces. The experimentally measured external wall surface temperature of west wall, T_{ex}, is considered as the outcome of the synthesis of ambient surroundings. The internal wall surfaces are cooled by convection q_{conv} between the induced air and the internal wall surface, as well as by the radiative heat transfer q_{rad} from the inner surface of the west wall to all internal surfaces of other walls simultaneously. T_{in}, denotes the internal surface temperature of the west wall, which has also been measured from the experimental setup in Section 2.1. Besides, as mentioned in Section 2.1 each wall consists of four material layers, where j (j=1,2,3,4) refers to the j^{th} layer of wall material.

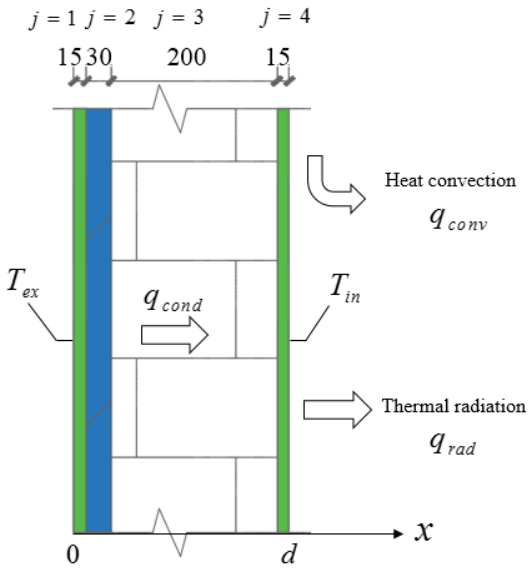

Fig.5. Schematic representation of heat transfers on the west wall during the night ventilation period.

For evaluation of the convection intensity of night ventilation schemes, we follow the approach recommended by Artmann [50] to acquire the transient convective heat flux at the internal surface of a wall as the difference between the conductive and radiative heat fluxes:

$$q_{conv}(\tau) = q_{cond}(\tau)\big|_{j=4} - q_{rad}(\tau) \quad (1)$$

where τ is the time. It should be noted that the conductive heat flux at the internal wall surface, $q_{cond}\big|_{j=4}$, refers to the heat flow through the 4th material layer, i.e. the 15mm-thick internal cement layer. The conductive heat flux is to be discussed in section 2.2.2, while the radiative heat flux is to be considered in section 2.2.3.

2.2.2 Conduction model

In order to evaluate the conductive heat transfer through walls, a 1-D transient conductive heat transfer equation [51] for the west wall is established as:

$$\lambda \frac{\partial^2 T}{\partial x^2} = \rho c \frac{\partial T}{\partial \tau} \quad (2)$$

In practice, Eq. (2) needs to be solved in a discrete format. The time step $\Delta\tau$ is set to be 60 s, in accordance with the sampling period of the sensors during the experiments. The measured external wall surface temperature and internal wall surface temperature of the west wall at the time instant *k* are employed as boundary conditions for the heat conduction model (Eq.2):

For the external surface (*x=0*):

$$T(x,\tau)\big|_{x=0} = T_{ex}^{k} \quad (3)$$

For the internal surface (*x=d*):

$$T(x,\tau)\big|_{x=d} = T_{in}^{k} \tag{4}$$

For each case, the calculation during of the heat transfer process of walls is from 8:00 for 24 hours, thus the initial condition for Eq. (2) is the measured temperatures at 8:00:

$$T(x,\tau)\big|_{\tau=0,x=0} = T_{ex}^{8:00} \tag{5}$$

$$T(x,\tau)\big|_{\tau=0,x=d} = T_{in}^{8:00} \tag{6}$$

A finite difference model [51] using an implicit scheme is built to solve Eq. (2) for obtaining the spatial distribution of the time-varying temperatures. Fig. 6 shows the differential model of the west wall. It is assumed that the west wall is discretized into 52 differential computing layers with the grid size Δx of 5 mm as illustrated in Fig. 6(a), and the grid *m* shown in Fig. 6(b) corresponds to the m^{th} computing layer.

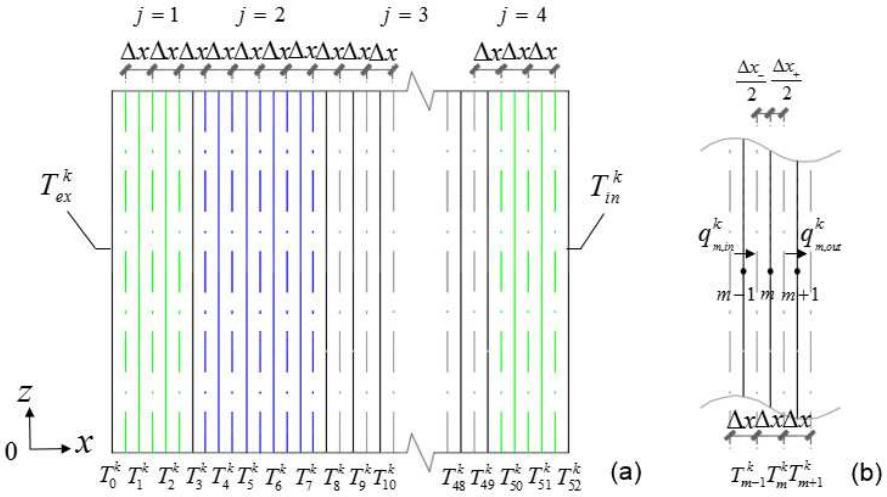

Fig. 6. Differential model of the west wall.

According to the energy balance analysis on the grid *m* as shown in Fig. 6(b), during time interval $\Delta\tau$, the increment of the internal energy heat of the grid m, Δq_m^k, equals to the difference between the heat absorbed from the left grid $m-1$ into the grid m, $q_{m,in}^k$ and the heat removed from the grid

m to the right grid $m+1$, $q^k_{m,out}$:

$$\Delta q^k_m = q^k_{m,in} - q^k_{m,out} \tag{7}$$

The increment of the internal energy heat Δq^k_m on the left-hand-side of Eq. (7) is calculated as:

$$\Delta q^k_m = \rho_{m,-}c_{m,-}\frac{\Delta x_-}{2}\frac{\partial T^k_m}{\partial \tau} + \rho_{m,+}c_{m,+}\frac{\Delta x_+}{2}\frac{\partial T^k_m}{\partial \tau} = (\rho_{m,-}c_{m,-} + \rho_{m,+}c_{m,+})\frac{\Delta x}{2}\frac{\partial T_m}{\partial \tau} \approx (\rho_{m,-}c_{m,-} + \rho_{m,+}c_{m,+})\frac{\Delta x}{2}\frac{T^k_m - T^{k-1}_m}{\Delta \tau} \tag{8}$$

The heat injected into the grid m is:

$$q^k_{m,in} = -\bar{\lambda}_- \frac{T^k_m - T^k_{m-1}}{\Delta x_-} \tag{9}$$

The heat removed from the grid m is:

$$q^k_{m,out} = -\bar{\lambda}_+ \frac{T^k_{m+1} - T^k_m}{\Delta x_+} \tag{10}$$

where $\rho_{m,-}$ and $\lambda_{m,-}$ are the density and thermal conductivity of the left half of grid m, $\rho_{m,+}$ and $\lambda_{m,+}$ are the density and thermal conductivity of the right half of grid m, λ_{m-1} and λ_{m+1} are the thermal conductivity of grids $m-1$, m and $m+1$, respectively. $\bar{\lambda}_- = \frac{2\lambda_{m-1}\lambda_m}{\lambda_{m-1}+\lambda_m}$ and $\bar{\lambda}_+ = \frac{2\lambda_m\lambda_{m+1}}{\lambda_m+\lambda_{m+1}}$ are the harmonic mean values of thermal conductivity.

After substituting Eqs. 8-10 into Eq. 7 with an implicit scheme, the new energy balance equation for the grid m at the junction of two material layers is obtained as:

$$T^k_m = -\frac{2\Delta\tau\bar{\lambda}_-}{(\rho_{m,-}c_{m,-} + \rho_{m,+}c_{m,+})\Delta x^2}T^{k+1}_{m-1} + \left[1 + \frac{2\Delta\tau(\bar{\lambda}_- + \bar{\lambda}_+)}{(\rho_{m,-}c_{m,-} + \rho_{m,+}c_{m,+})\Delta x^2}\right]T^{k+1}_m - \frac{2\Delta\tau\bar{\lambda}_+}{(\rho_{m,-}c_{m,-} + \rho_{m,+}c_{m,+})\Delta x^2}T^{k+1}_{m+1} \tag{11}$$

For the grid in the same material layer of uniform thermal parameters, $\overline{\lambda}_{-}=\overline{\lambda}_{+}=\lambda_m$, and the new energy balance equation then becomes:

$$T_m^k=-\frac{\lambda_m}{\rho_m c_m}\cdot\frac{\Delta\tau}{\Delta x^2}T_{m-1}^{k+1}+\left[1+\frac{2\lambda_m}{\rho_m c_m}\cdot\frac{\Delta\tau}{\Delta x^2}\right]T_m^{k+1}-\frac{\lambda_m}{\rho_m c_m}\cdot\frac{\Delta\tau}{\Delta x^2}T_{m+1}^{k+1} \tag{12}$$

By introducing the thermal diffusivity $a_m=\frac{\lambda_m}{\rho_m c_m}$, the Fourier number $Fo_m=\frac{a_m\Delta\tau}{\Delta x^2}$, $XF_{-}=\frac{2\Delta\tau\overline{\lambda}_{-}}{(\rho_{m,-}c_{m,-}+\rho_{m,+}c_{m,+})\Delta x^2}$ and $XF_{+}=\frac{2\Delta\tau\overline{\lambda}_{+}}{(\rho_{m,-}c_{m,-}+\rho_{m,+}c_{m,+})\Delta x^2}$, Eq. (11) and Eq. (12) can be rewritten as:

$$T_m^k=-XF_{-}T_{m-1}^{k+1}+(1+XF_{-}+XF_{+})T_m^{k+1}-XF_{+}T_{m+1}^{k+1} \tag{13}$$

$$T_m^k=-Fo_mT_{m-1}^{k+1}+(1+2Fo_m)T_m^{k+1}-Fo_mT_{m+1}^{k+1} \tag{14}$$

Finally, the temperature distribution at the grid m of the west wall, T_m^k, at the time instant k is obtained by solutions of the following equation:

$$\begin{cases}
T_1^k=-Fo_1T_0^{k+1}+(1+2Fo_1)T_1^{k+1}-Fo_1T_2^{k+1}\\
T_2^k=-Fo_2T_1^{k+1}+(1+2Fo_2)T_2^{k+1}-Fo_2T_3^{k+1}\\
T_3^k=-XF_2T_2^{k+1}+(1+XF_2+XF_4)T_3^{k+1}-XF_4T_4^{k+1}\\
T_4^k=-Fo_4T_3^{k+1}+(1+2Fo_4)T_4^{k+1}-Fo_4T_5^{k+1}\\
\cdots\cdots\\
T_7^k=-Fo_7T_6^{k+1}+(1+2Fo_7)T_7^{k+1}-Fo_7T_8^{k+1}\\
T_8^k=-XF_7T_7^{k+1}+(1+XF_7+XF_9)T_8^{k+1}-XF_9T_9^{k+1}\\
T_9^k=-Fo_9T_8^{k+1}+(1+2Fo_9)T_9^{k+1}-Fo_9T_{10}^{k+1}\\
\cdots\cdots\\
T_{48}^k=-Fo_{48}T_{47}^{k+1}+(1+2Fo_{48})T_{48}^{k+1}-Fo_{48}T_{49}^{k+1}\\
T_{49}^k=-XF_{48}T_{48}^{k+1}+(1+XF_{48}+XF_{50})T_{49}^{k+1}-XF_{50}T_{50}^{k+1}\\
T_{50}^k=-Fo_{50}T_{49}^{k+1}+(1+2Fo_{50})T_{50}^{k+1}-Fo_{50}T_{51}^{k+1}\\
T_{51}^k=-Fo_{51}T_{50}^{k+1}+(1+2Fo_{51})T_{51}^{k+1}-Fo_{51}T_{52}^{k+1}
\end{cases} \tag{15}$$

Eq. (15), the finite-difference formulation of Eq. (2), is solved using Crank–Nicholson time stepping method with the measured internal and external wall temperatures as boundary conditions. This results in the transient temperature distribution within a multi-layer wall. At each time step during the night ventilation period, the conductive heat flux density, $q_{cond,j}^{k}$ through the j^{th} material layer of the west wall at time instant *k*, can then be obtained from Fourier's law:

$$q_{cond,j}^{k} = \lambda_j \frac{T_{ex,j}^{k} - T_{in,j}^{k}}{d_j} \tag{16}$$

where $T_{ex,j}^{k}$ is the external surface temperature of the j^{th} layer of wall material, $T_{in,j}^{k}$ is the internal surface temperature of the j^{th} layer of wall material, d_j and λ_j are the thickness and thermal conductivity of the j^{th} layer of wall material, respectively.

2.2.3 Radiation model of wall surfaces

During the night ventilation, the radiative heat flux is related to temperature differences between the inner wall surfaces. The radiation model assumes that the inner surfaces of the envelope are diffuse-grey surfaces and six surfaces form an enclosure. Besides, room air is a non-participating medium. The total radiation leaves the radiant surface s per unit time and per unit surface area, J_s is calculated using Eq. (17). The net radiative heat flux $q_{rad,s}$ from the grey-body surface s to all five other surfaces p is then obtained from Eq. (18), which is defined as the difference between the radiations leaving and arriving the surface s :

$$J_s = \varepsilon_s \cdot \sigma \cdot T_s^4 + (1-\varepsilon_s)\sum_{p=1}^{6} F_{s,p} J_p , \qquad s = 1,2,...,6 \tag{17}$$

$$q_{rad,s} = J_s - \sum_{p=1}^{6} F_{s,p} J_p , \qquad s = 1,2,...,6 \tag{18}$$

where ε_s is the emissivity of surface s, σ is the Stefan-Boltzmann constant, T_s denotes the average of the thermocouple readings at the internal surface of wall s, *and* $F_{s,p}$ stands for the view factor from surface s to surface p.

3. Results and discussion

In this section, the experimental results are first presented and discussed, focusing on the cooling effects of night ventilation schemes on wall surface temperatures and room air temperature. The results of the theoretical models discussed in Section 2.2 are also analyzed including the enhanced convection over the wall surface and the heat removal from walls. Finally, the performance evaluation indices are employed to assess the cooling efficiency and energy efficiency of night ventilation with WAV.

3.1. Experimental results and analyses

3.1.1 Wall surface temperature

Fig. 7 shows the experimental results of the time-varying external wall surface temperatures and internal wall surface temperatures of the three cases investigated. Each curve is obtained by averaging the measurements from all thermocouples attached on the same wall surface (five thermocouples for each surface). Furthermore, moving average of every five minutes (five data points) has been applied so as to reduce the influence from measurement noise on the results. As seen in Fig. 7, the similar tendency of the measured external wall surface temperatures in these three cases again verifies that the selected three cases have similar outdoor weather conditions, in accordance with the results in Fig. 3. The relatively high-frequency fluctuations of external surface temperatures of the west wall in the

afternoon are mainly due to the cloudy weather conditions. In Case 1 as shown in Fig. 7(a), an evident decrease of the internal surface temperature of the west wall is observed from 22:00 when it starts to apply the WAV system on this wall. It is interesting to note that the internal surface temperatures of other three walls also decrease with the application of WAV on the west wall. The gap between the external wall surface temperature and the internal wall surface temperature becomes significantly narrowed when WAV is switched on. However, due to the heating effect of the fan and the cooling loss during transportation, the internal wall surface temperatures are still always higher than the external wall surface temperatures. In Case 2 with natural night ventilation shown in Fig. 7(b), a slight decrease of internal wall surface temperatures is also observed from 22:00 when natural ventilation is started. However, although the outdoor air temperatures at daytime in Case 2 are slightly lower than that in Case 1, the internal wall surface temperatures of are much higher than that in Case 1 at nighttime. This clearly reveals the superior performance of WAV on night cooling than natural ventilation. In Case 3 without ventilation (Fig. 7(c)), the outdoor air temperature decreases after 20:00. Nevertheless, the internal wall surface temperatures still increase slowly and reach 35 ℃, which indicates that the heat dissipation of structural mass during the night has bad influence on the indoor climate. Comparing the experimental results of wall surface temperatures of these three cases, it is found that the internal wall surface temperatures of Case 1 with WAV are approximately 5 ℃ lower than the cases without WAV, which proves that the WAV system has a significant temperature decreasing effect on internal walls.

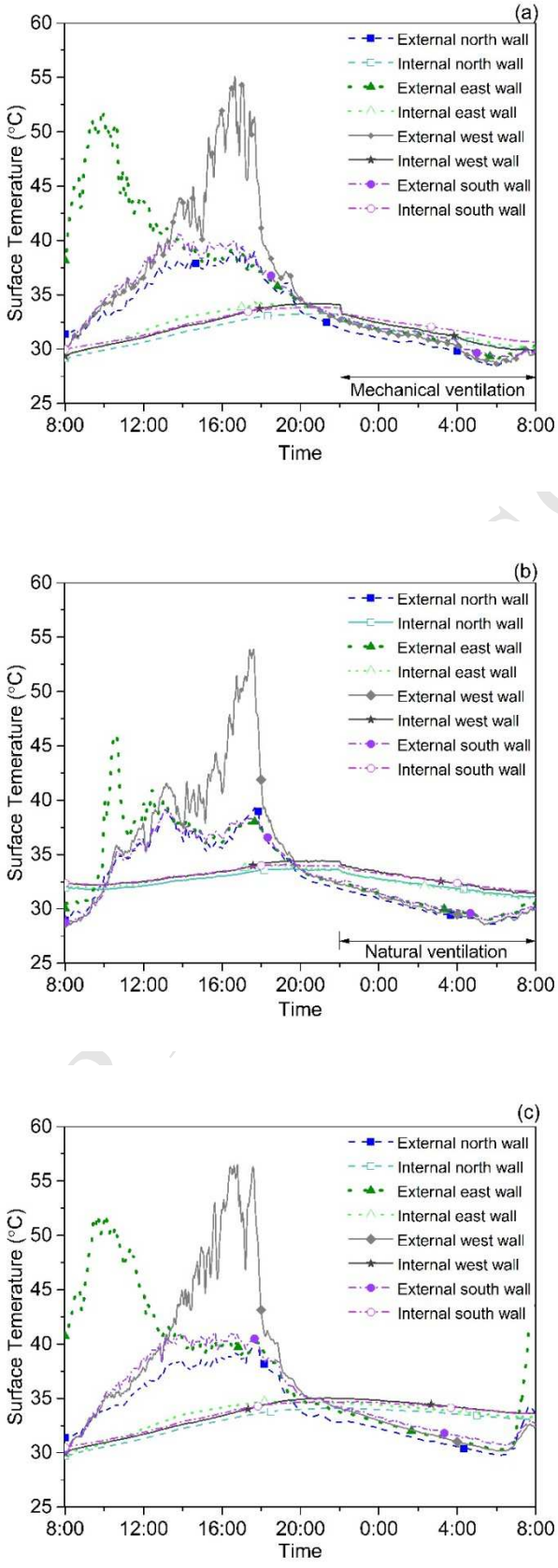

Fig. 7. Measured external and internal wall surface temperatures. (a) Case 1: WAV from 22:00 to 8:00, ACR = 10.27 ACH;

(b) Case 2: Natural night ventilation from 22:00 to 8:00, ACR = 1.14 ACH; (c) Case 3: no ventilation for 24 hours. For interpretation of the references to color in this figure legend, the reader is referred to the web version of the article.

3.1.2. Room air temperature

Fig. 8 illustrates the mean values and standard deviations (based on measurements from the five thermocouples at different locations of the central plane as shown in Fig. 4(b)) of the room air temperatures in the three cases. Compared with the Case 3, an obvious decline of the room air temperature is observed with the application of night ventilation in both Case 1 and Case 2, and the WAV system further exhibits a much better performance in cooling the room air temperature than natural night ventilation. Furthermore, from 22:00 to 4:00 at nighttime, the standard deviations of the room air temperature with WAV (Case 1) are very small, indicating the indistinctive differences between the five monitored room air temperatures at the central plane. It should be noted here that to further reveal the room air temperature distribution, more evidences are needed, e.g. measuring air temperature distribution at least at three vertical sections parallel to the wall with WAV, monitoring ventilation rate in the room. These should be considered in the further study. Then, after 4:00 the standard deviation of the room air temperature starts to increase. This non-isothermal condition of room air temperature starting from 4:00 might be explained by the fact that the eastern part of the room is warmed with the increasing outdoor air temperature due to sunrise, while the western part is still cooled by ventilation. The standard deviations in Case 2 are also reduced for a very short period after 22:00 by the natural night ventilation, but soon increase to relatively large values for the remaining nighttime. Furthermore, the standard deviations in Case 3 are rather constant with relatively small values, due to the insignificant air circulation in the closed chamber.

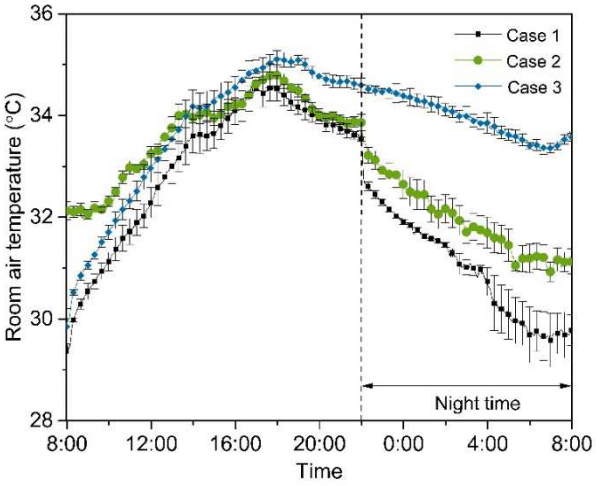

Fig. 8. Mean values and standard deviations of the measured room air temperatures in the three different cases.

3.2 Results of thermal analyses

3.2.1 Conductive heat flux of the walls

Fig. 9. shows the time-varying conductive heat flux through the west wall from 22:00 to 8:00. In this paper, the heat injected into the room through the wall is defined positive and the heat removed from the room is defined negative. From 22:00 to 6:00, the conductive heat flux at internal cement layer is positive, while the conductive heat flux of external cement layer in all three cases is negative. This implies that the heat is dissipated from the internal wall surface to the room, and that at the meantime, the heat is also released from the external wall surface to the surroundings. When WAV is switched on at 22:00 in Case 1, an initial steep increase of the conductive heat flux through the internal cement is observed. Afterwards, the heat flux of the internal cement reaches the quasi-steady state quickly. In Case 2, the starting up of natural ventilation has a slight influence (enhancement) on the heat flow in the wall materials. Due to the circulation of room air driven by the natural night ventilation, the

heat flux of the internal cement is fluctuating around a constant positive value. In Case 3, the conductive heat flux of the internal cement is still positive but smaller than those in the other two cases, indicating that the heat stored in the walls is still released into the indoor environment. However, without outlet openings to exhaust the heat in the room, the cooling of the room and the walls only relies on the heat dissipating through the walls to the outdoor environment. After 6:00 the next morning when the sun rises, the conductive heat flux of the external cement increases dramatically in Case 3. On the other hand, due to the precooling effect of night ventilation, the heat flow rates of the external cement layer in Case 1 and Case 2 rise slowly, and thus the temperature increase of the whole room is delayed.

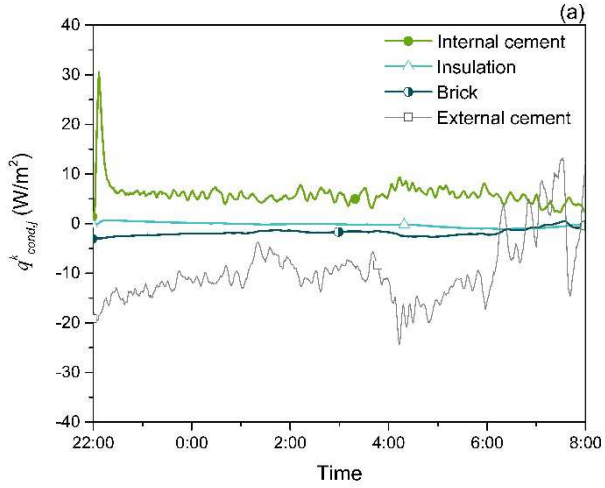

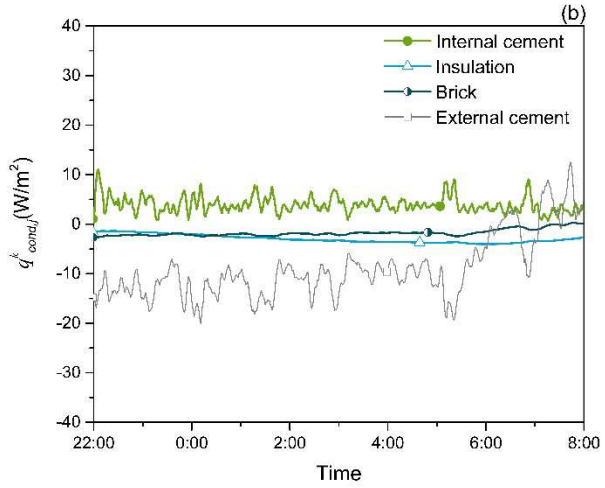

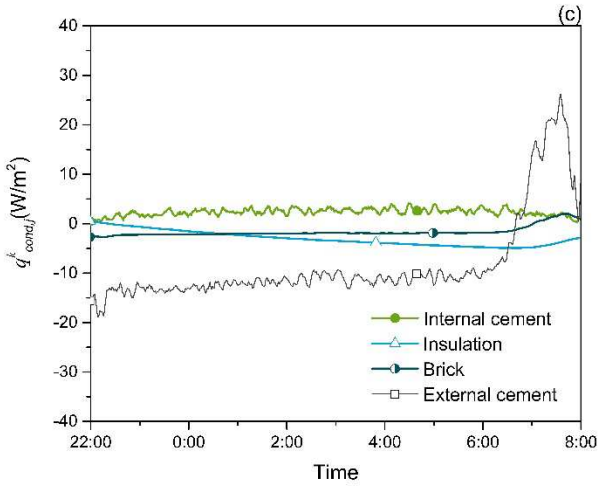

Fig. 9. Conductive heat flux $q^k_{cond,j}$ (W/m^2) of west walls. (a) Case 1: WAV from 22:00 to 8:00, ACR = 10.27 ACH; (b) Case 2: Natural night ventilation from 22:00 to 8:00, ACR = 1.14 ACH; (c) Case 3: no ventilation. For interpretation of the references to color in this figure legend, the reader is referred to the web version of the article.

3.2.2. Convective heat flux of ventilated wall with WAV during night cooling period

Fig.10 shows the calculated instantaneous internal surface convection, q_{conv} of the west wall with the WAV system (Case 1) for eight hours (22:00-6:00). Also, the picture depicts the measured temperatures including the inlet air temperature T_{inlet}, the internal surface temperature of the west wall T_{in}, the room air temperature T_{room} and the outlet air temperature T_{outlet}. During the night ventilation period, the room air and the wall surface are simultaneously cooled in proportion to the decrease of the supply air temperature. As for the convective heat flux, an initial steep transition (steep increase followed by a steep decrease) is observed in the first twenty minutes resulting from the start-up of night ventilation. After that, the quasi-steady state is soon reached with slight fluctuations for the rest of the ventilation period, due to the steady heat transfer process. In addition, the calculated convective heat flux from 4:00 to 6:00 is slightly higher than its average value. The main reason is

that during this period the outdoor air temperatures become relatively low, and thus the walls can be further cooled by night ventilation.

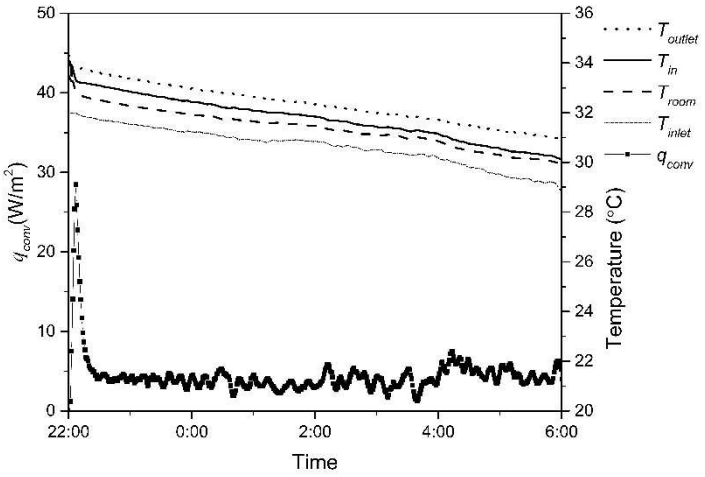

Fig. 10. The convective heat flux at internal surface of the west wall and the measured temperatures. Case 1: WAV from 22:00 to 8:00, ACR = 10.27 ACH

In general, the convective heat transfer coefficient (CHTC) is related to the mechanism of airflow and the geometry of the specific system [52]. Since the air velocities and temperatures are not uniformly distributed on the wall, the CHTC values are different at different points on the wall. Nevertheless, for revealing the overall performance of the WAV system, the overall average of CHTC, $\overline{h}$, is calculated using Newton's Cooling Law:

$$\overline{h} = \overline{q}_{conv} / (\overline{T}_{in} - \overline{T}_{room}) \quad (19)$$

where $\overline{q}_{conv}$, $\overline{T}_{in}$ and $\overline{T}_{room}$ are the average values (both time- and spatial- averaged) of the convective heat flux, the internal west-wall surface temperature and the room air temperature,

respectively. Using Eq. (19), the overall average value of CHTC at the west wall during the night turns out to be 10.79 W m^{-2} ℃$^{-1}$, indicating that the WAV system results in a high value of CHTC, which enables effective temperature decreasing of the test chamber.

3.2.3. Heat removal amount

In general, as a low-energy cooling strategy, night ventilation functions by generating a time lag between heat gains and heat losses, as well as reducing the cooling load needed in the following day. As mentioned in Section 1, the wall materials are considered as the primary elements of thermal mass in this study, since the contributions from the roof (the heat capacity of the roof material is low according to Table 1), floor and internal objects can be neglected. The thermal storage capacity of the wall depends on: (1) the thermal properties of each material layer, (2) its thickness, (3) the heat transfer at the wall surfaces and (4) the difference between the outdoor air temperature and the indoor air temperature. In order to evaluate the heat removal effect, the amount of heat increment of each layer *j* of the west wall is integrated resulting in the total heat removal from the west wall, Q_w:

$$Q_w(\tau) = A_w \sum_{j=1}^{4} c_j \rho_j d_j \Delta T_j(\tau) \quad (20)$$

where A_w *is* the surface area of the west wall, c_j, ρ_j, and d_j are the thermal conductivity, density and thickness of the j^{th} layer of wall material, respectively. $\Delta T_j(\tau)$ is the temperature increment of the j^{th} layer of wall material, i.e. the difference between the present temperature with respect to its temperature at 22:00.

Fig. 11 shows the accumulated heat removal from the west wall during the night for the three cases. A negative Q_w indicates that the heat is removed from the wall. The heat removal amount of the west wall without ventilation in Case 3 is taken as a reference. With natural ventilation (Case 2), a slight increase of heat dissipation is observed, which proves that in the natural convection regime, the heat stored in walls cannot be sufficiently removed. With WAV, the amount of heat removed from the wall is dramatically increased, i.e. about five times as much as that in Case 1 and Case 2, demonstrating the high effectiveness of heat extraction with the WAV system.

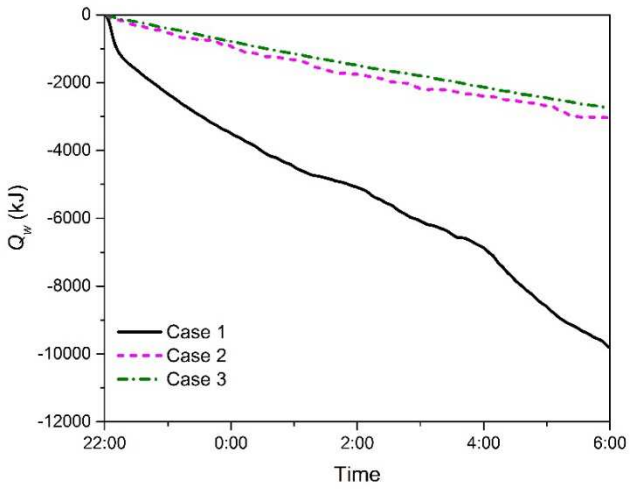

Fig. 11. Accumulative heat removals from the west wall. Case 1: WAV from 22:00 to 8:00, ACR = 10.27 ACH; Case 2: Natural night ventilation from 22:00 to 8:00, ACR = 1.14 ACH; Case 3: no ventilation.

In addition, the heat extracted from the whole test chamber (contributions from the four walls) per hour $Q_{extr,perhour}$ during the night time is calculated and presented in Fig. 12. Limited improvement of the amount of hourly heat extraction in Case 2 is observed comparing with Case 3. In contrast, the WAV system leads to significant enhancement of the hourly heat removal especially at two durations: the first ventilated hour (22:00-23:00) and the duration with relatively low outdoor air temperature (4:00-6:00).

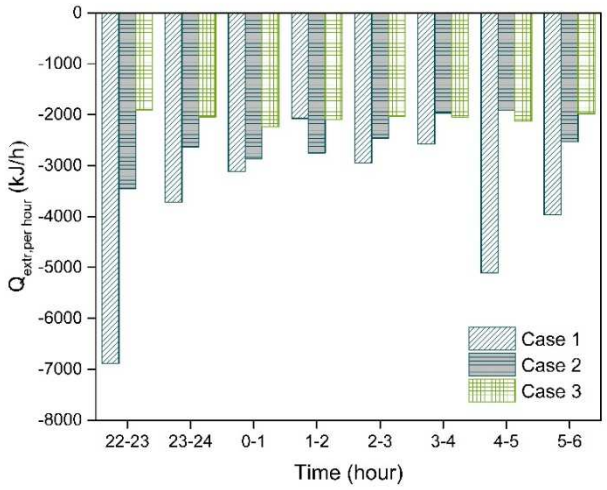

Fig. 12. Hourly values of heat extraction from the whole chamber during the night time.

Finally, the total amount of heat dissipation for the whole chamber from 22:00 to 6:00, Q_{extr}, is also calculated for these three cases. The calculated values of Q_{extr} are 30835 kJ, 20834 kJ and 16704 kJ for Case 1, Case 2 and Case 3, respectively. Hence, WAV results in approximately double amount of heat dissipation compared with the non-ventilation case and about 1.5 times amount compared with the natural ventilation case. This is because the predominate forced convection in the WAV system enhances the efficiency of heat removal.

3.3. Performance indices of WAV

3.3.1. Surface cooling effectiveness

The surface cooling effectiveness η_{surf} recommended by Artmann [50] has been employed in the present study:

$$\eta_{surf} = \frac{T_{outlet} - T_{inlet}}{\overline{T}_{surf} - T_{inlet}}$$

(21

)

where T_{inlet} is the inlet air temperature, and $\overline{T}_{surf}$ is the hourly average value of all surface temperatures.

As shown in Fig. 13, the hourly surface cooling effectiveness of WAV (Case 1) declines as the difference between the outdoor air temperature and indoor air temperature decreases. Excluding the first ventilated hour (in order to eliminate the initial transient effect), the overall average value of the hourly surface cooling effectiveness of WAV during the night ventilation is calculated to be 1.48. According to Artmann et al. [50], the surface cooling effectiveness of both DV and MV with the same air change rate is about 0.8, indicating that WAV exhibits a better surface cooling performance than DV and MV.

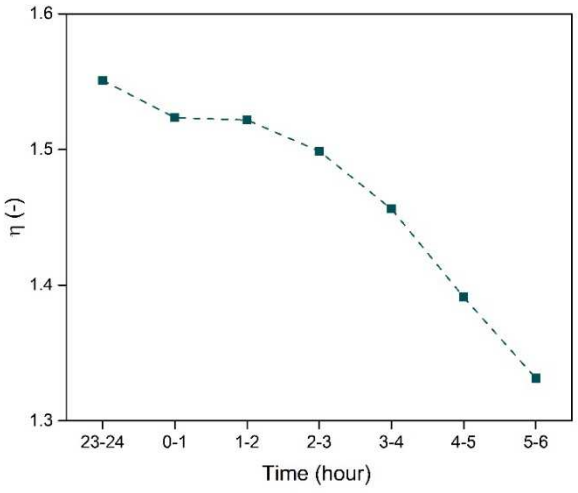

Fig. 13. Surface cooling effectiveness η_{surf} of WAV. Hourly mean values, first ventilated hour excluded.

3.3.2. Night ventilation effectiveness

The performance on heat removal of night cooling systems can also be described using the night ventilation effectiveness, η_{vent}, which is the ratio of cooling amount provided by ventilation Q_{vent} and the total heat extraction amount from the chamber Q_{extr} (calculated in section 3.2.3):

$$\eta_{vent} = \frac{Q_{vent}}{Q_{extr}} \tag{22}$$

$$Q_{vent} = c_a \dot{m} (T_{outlet} - T_{inlet}) \tag{23}$$

In Eq. (23), c_a is the thermal conductivity of room air, and $\dot{m}$ is the mass flow of supply air. Using Eq. (22), the calculated night ventilation effectiveness with the WAV system is 0.153. As can be seen from Fig.5, the test chamber is not adiabatic, thus both the heat dissipation by the outdoor environment and heat extraction by the indoor night ventilation contribute to the temperature decreasing effect on walls during the night.

3.3.3. Energy consumption analysis

Coefficient of performance (COP) of the WAV system is defined as:

$$\mathrm{COP} = \frac{Q_{extr}}{Q_{fan}} \tag{24}$$

)

where Q_{extr} has been calculated in section 3.2.3, and Q_{fan} is the fan power consumption as presented in Table 2.

During the calculation period from 22:00 to 6:00, the overall COP of the WAV system is 26.8, indicating that WAV can achieve extraordinary performance on energy saving with a low level of fan power consumption.

4. Conclusions and outlook

In this study, thermal performance of the novel WAV system for night cooling of an office-type room under hot summer conditions were investigated by both chamber experiment and theoretical model. The thermal performance of cases with WAV, with natural ventilation and without ventilation were compared, in terms of the effect on the temperature decreasing and heat removal. Three different performance indices were also used to further reveal the performance of night ventilation with WAV. From this study, the following conclusions can be drawn:

The measured temperature fields show that the WAV scheme results in a better temperature decreasing effect on both the wall surfaces and the room air, comparing with the natural night ventilation. Although WAV is only applied to the west wall, the internal surface temperatures of the other three walls are also slightly lowered, implying a superior performance of WAV on cooling the whole room.

Based on the results of the established heat transfer model, it is seen that the enhanced convection between the induced air and the internal wall surface is achieved. With WAV, the amount of heat

removed from the ventilated wall is about five times that in the natural night ventilation case or non-ventilation case. Moreover, WAV results in approximately double amount of heat dissipation from the whole chamber compared with the non-ventilation case, and about 1.5 times amount compared with the natural ventilation case.

The surface cooling effectiveness, night ventilation effectiveness and COP were calculated. The average values of the surface cooling effectiveness and the night ventilation effectiveness of WAV are 1.48 and 0.153, respectively, indicating that night ventilation with WAV performs efficiently in temperature decreasing and heat removal. The overall COP of WAV turns out to be 26.8, and this large value demonstrates the high energy saving potential of the WAV system with a low level of initial cost of ventilation facilities.

This study is limited to the thermal performance comparisons of WAV with natural night ventilation (and non-ventilation as well), and comparisons with other types of air distribution methods need to be performed in the future. Further studies on different airflow rates, multi-heat sources in a room and thermophysical properties of walls (such as using PCM) are also beneficial for revealing more possibilities and limitations of WAV.

Acknowledgements

The authors wish to express their appreciation for the financial support from the National Natural Science Foundation of China (NSFC) (51578086, 51806022) and Aarhus University Research Foundation under the AUFF Assistant Professor Starting Grant (AUFF-E-2017-7-20).

References

[1] International Energy Agency, Energy Technology Perspectives: Scenarios & Strategies To 2050, 2010. doi:10.1049/et:20060114.

[2] Tsinghua University Buildings Energy Efficiency Research Center, 2017 annual report on China building energy efficiency, China Architecture and BuildingPress, Beijing, 2017.

[3] Y. Zhang, C.-Q. He, B.-J. Tang, Y.-M. Wei, China's energy consumption in the building sector: A life cycle approach, Energy Build. 94 (2015) 240–251. doi:10.1016/j.enbuild.2015.03.011.

[4] V. Geros, M. Santamouris, A. Tsangrasoulis, G. Guarracino, Experimental evaluation of night ventilation phenomena, Energy Build. 29 (1999) 141–154. doi:10.1016/S0378-7788(98)00056-5.

[5] J. Pfafferott, S. Herkel, M. Jäschke, Design of passive cooling by night ventilation: Evaluation of a parametric model and building simulation with measurements, Energy Build. 35 (2003) 1129–1143. doi:10.1016/j.enbuild.2003.09.005.

[6] M. Kolokotroni, A. Aronis, Cooling-energy reduction in air-conditioned offices by using night ventilation, Appl. Energy. 63 (1999) 241–253. doi:10.1016/S0306-2619(99)00031-8.

[7] O. Irulegi, A. Ruiz-Pardo, A. Serra, J.M. Salmeron, Potential of night ventilative cooling strategies in office buildings in Spain - Comfort analysis, Int. J. Vent. 13 (2014) 193–210. doi:10.1080/14733315.2014.11684048.

[8] T. Kubota, D.T.H. Chyee, S. Ahmad, The effects of night ventilation technique on indoor thermal environment for residential buildings in hot-humid climate of Malaysia, Energy Build. 41 (2009) 829–839. doi:10.1016/j.enbuild.2009.03.008.

[9] L. Yang, Y. Li, Cooling load reduction by using thermal mass and night ventilation, Energy Build. 40 (2008) 2052–2058. doi:10.1016/j.enbuild.2008.05.014.

[10] N. Artmann, H. Manz, P. Heiselberg, Parameter study on performance of building cooling by night-time ventilation, Renew. Energy. 33 (2008) 2589–2598. doi:10.1016/j.renene.2008.02.025.

[11] S.P. Corgnati, A. Kindinis, Thermal mass activation by hollow core slab coupled with night ventilation to reduce summer cooling loads, Build. Environ. 42 (2007) 3285–3297. doi:10.1016/j.buildenv.2006.08.018.

[12] P. Phelan, Coupling of thermal mass with night ventilation in buildings, ARIZONA STATE UNIVERSITY, 2011.

[13] G. Zhou, Y. Yang, H. Xu, Energy performance of a hybrid space-cooling system in an office building using SSPCM thermal storage and night ventilation, Sol. Energy. 85 (2011) 477–485. doi:10.1016/j.solener.2010.12.028.

[14] G. Zhou, Y. Yang, X. Wang, S. Zhou, Numerical analysis of effect of shape-stabilized phase change material plates in a building combined with night ventilation, Appl. Energy. 86 (2009) 52–59. doi:10.1016/j.apenergy.2008.03.020.

[15] Y. Wang, F.Y. Zhao, J. Kuckelkorn, X.H. Li, H.Q. Wang, Indoor air environment and night cooling energy efficiency of a southern German passive public school building operated by the heat recovery air conditioning unit, Energy Build. 81 (2014) 9–17. doi:10.1016/j.enbuild.2014.06.008.

[16] J. Zhou, G. Zhang, Y. Lin, Y. Li, Coupling of thermal mass and natural ventilation in buildings, Energy Build. 40 (2008) 979–986. doi:10.1016/j.enbuild.2007.08.001.

[17] B. Givoni, Comfort, climate analysis and building design guidelines, Energy Build. 18 (1992) 11–23. doi:10.1016/0378-7788(92)90047-K.

[18] N. Artmann, H. Manz, P. Heiselberg, Climatic potential for passive cooling of buildings by night-time ventilation in Europe, Appl. Energy. 84 (2007) 187–201. doi:10.1016/j.apenergy.2006.05.004.

[19] X. Qi, Cooling potential and applicability of night ventilation on office buildings in North China (In Chinese), Xi'an University of Architecture and Technology, 2009.

[20] China Planning Press, Code for Thermal Design of Civil Building(GB 50176-2016), Beijing, 2006.

[21] J.C. Lam, L. Yang, J. Liu, Development of passive design zones in China using bioclimatic approach, Energy Convers. Manag. 47 (2006) 746–762. doi:10.1016/j.enconman.2005.05.025.

[22] Yang Liu, Climatic Analysis and Architectural Design Strategies for Bio-Climatic Design (in Chinese), Xi'an University of Architecture and Technology, 2003.

[23] S. Leenknegt, R. Wagemakers, W. Bosschaerts, D. Saelens, Numerical study of convection during night cooling and the implications for convection modeling in Building Energy Simulation models, Energy Build. 64 (2013) 41–52. doi:10.1016/j.enbuild.2013.04.012.

[24] P. Roach, F. Bruno, M. Belusko, Modelling the cooling energy of night ventilation and economiser strategies on façade selection of commercial buildings, Energy Build. 66 (2013) 562–570. doi:10.1016/j.enbuild.2013.06.034.

[25] Q. Chen, Ventilation performance prediction for buildings: A method overview and recent applications, Build. Environ. 44 (2009) 848–858. doi:10.1016/j.buildenv.2008.05.025.

[26] J. Le Dréau, P. Heiselberg, R.L. Jensen, Experimental investigation of convective heat transfer during night cooling with different ventilation systems and surface emissivities, Energy Build. 61 (2013) 308–317. doi:10.1016/j.enbuild.2013.02.021.

[27] S. Leenknegt, R. Wagemakers, W. Bosschaerts, D. Saelens, Numerical sensitivity study of transient surface convection during night cooling, Energy Build. 53 (2012) 85–95. doi:10.1016/j.enbuild.2012.06.020.

[28] J.M.S. Lissen, J.A.S. Fernández, F.J.S. de la Flor, S.Á. Domínguez, Á.R. Pardo, Flow pattern effects on night cooling ventilation, Int. J. Vent. 6 (2007) 21–30. doi:10.1080/14733315.2007.11683761.

[29] J. Landsman, Performance, Prediction and Optimization of Night Ventilation across Different Climates, 2017.

[30] D. Müller, C. Kandzia, R. Kosonen, A.K. Melikov, P. V. Nielsen, Mixing Ventilation. Guide on mixing air distribution design, REHVA Guidebook No.19, 2013.

[31] S.E. Grigorescu, N. Petkov, P. Kruizinga, a Comparison Between Four Different Ventilation Systems, IEEE Trans. Image Process. 11 (2002) 1160–7. doi:10.1109/TIP.2002.804262.

[32] T. Karimipanah, H.B. Awbi, M. Sandberg, C. Blomqvist, Investigation of air quality, comfort parameters and effectiveness for two floor-level air supply systems in classrooms, Build. Environ. 42 (2007) 647–655. doi:10.1016/j.buildenv.2005.10.016.

[33] H.J. Chen, B. Moshfegh, M. Cehlin, Numerical investigation of the flow behavior of an isothermal impinging jet in a room, Build. Environ. 49 (2012) 154–166. doi:10.1016/j.buildenv.2011.09.027.

[34] H.J. Chen, B. Moshfegh, M. Cehlin, Investigation on the flow and thermal behavior of impinging jet ventilation systems in an office with different heat loads, Build. Environ. 59 (2013) 127–144. doi:10.1016/j.buildenv.2012.08.014.

[35] H. Chen, S. Janbakhsh, U. Larsson, B. Moshfegh, Numerical investigation of ventilation

performance of different air supply devices in an office environment, Build. Environ. 90 (2015) 37–50. doi:10.1016/j.buildenv.2015.03.021.

[36] Y. Cho, H.B. Awbi, T. Karimipanah, Theoretical and experimental investigation of wall confluent jets ventilation and comparison with wall displacement ventilation, Build. Environ. 43 (2008) 1091–1100. doi:10.1016/j.buildenv.2007.02.006.

[37] S. Janbakhsh, B. Moshfegh, Experimental investigation of a ventilation system based on wall con fl uent jets, Build. Environ. 80 (2014) 18–31. doi:10.1016/j.buildenv.2014.05.011.

[38] H. Andersson, M. Cehlin, B. Moshfegh, Experimental and numerical investigations of a new ventilation supply device based on confluent jets, Build. Environ. 137 (2018) 18–33. doi:10.1016/j.buildenv.2018.03.038.

[39] T. Karimipanah, H.B. Awbi, Theoretical and experimental investigation of impinging jet ventilation and comparison with wall displacement ventilation, Build. Environ. 37 (2002) 1329–1342. doi:10.1016/S0360-1323(01)00117-2.

[40] T. Arghand, T. Karimipanah, H.B. Awbi, M. Cehlin, U. Larsson, E. Linden, An experimental investigation of the flow and comfort parameters forunder-floor, confluent jets and mixing ventilation systems in an open-plan office, Build. Environ. 92 (2015) 48–60. doi:10.1016/j.buildenv.2015.04.019.

[41] G. Cao, Modelling the attached plane jet in a room, Helsinki University of Technology, 2009.

[42] G. Cao, J. Kurnitski, M. Ruponen, O. Seppänen, Experimental investigation and modelling of a buoyant attached plane jet in a room, Appl. Therm. Eng. 29 (2009) 2790–2798. doi:10.1016/j.applthermaleng.2009.01.016.

[43] A. Li, H. Yin, W. Zhang, A novel air distribution method - Principles of air curtain ventilation,

Int. J. Vent. 10 (2012) 383–390. doi:10.1080/14733315.2012.11683963.

[44] A.G. Li, H.G. Yin, G.D. Wang, Experimental investigation of air distribution in the occupied zones of an air curtain ventilated enclosure, Int. J. Vent. 11 (2012) 171–182. doi:10.1080/14733315.2012.11683979.

[45] H.G. Yin, A.G. Li, Airflow characteristics by air curtain jets in full-scale room, J. Cent. South Univ. Technol. (English Ed. 19 (2012) 675–681. doi:10.1007/s11771-012-1056-8.

[46] H. Yin, A. Li, Study of attached air curtain ventilation within a full-scale enclosure: Comparison of four turbulence models, Indoor Built Environ. 25 (2016) 962–975. doi:10.1177/1420326X16655593.

[47] W. Ji, P. Heiselberg, H. Wang, Y. Hu, Z. Zhang, Experimental Assessment of Mechanical Night Ventilation on Inner Wall Surfaces, in: Proc. 12th REHVA World Congr., Aalborg, Denmark, 2016. http://vbn.aau.dk/files/233778874/paper_753.pdf.

[48] W. Ji, P.K. Heiselberg, Q. Luo, H. Wang, Z. Zhang, Experimental analysis on wall jet night ventilation system, in: Proc. Roomvent Vent., Espoo, Finland, 2018: pp. 433–438.

[49] W. Ji, Q. Luo, Z. Zhang, H. Wang, Cooling Effect of Mechanical Night Ventilation over Internal Wall Surface : A Parametric Analysis, in: Proc. 4th Int. Conf. Build. Energy Environ., Melbourne, Australia, 2018: pp. 457–461.

[50] N. Artmann, R.L. Jensen, H. Manz, P. Heiselberg, Experimental investigation of heat transfer during night-time ventilation, Energy Build. 42 (2010) 366–374. doi:10.1016/j.enbuild.2009.10.003.

[51] S. V. Patankar., Numerical Heat Transfer and Fluid Flow First ed., Hemisphere Publishing Corporation, Washington, New York, London, 1980.

[52] K. Goethals, H. Breesch, A. Janssens, Sensitivity analysis of predicted night cooling performance to internal convective heat transfer modelling, Energy Build. 43 (2011) 2429–2441. doi:10.1016/j.enbuild.2011.05.033.

Research highlights

- A novel wall-mounted attached ventilation (WAV) night cooling system proposed
- Experiments carried out to understand the temperature decreasing effect of WAV
- Transient heat transfer models established to analyse the thermal performance of WAV
- WAV has much better performance on surface cooling and heat removal than natural ventilation